Chapter 6
Tube Number Density Control of AAO Assisted CNT Arrays

6.1 Introduction

Carbon nanotubes (CNTs) have attracted much interest for their remarkable properties and diversified applications since they were discovered by Iijima[Iijima 1991-56]. In particular, CNTs have become one of the most promising candidates for field electron emitters to be used in future generations of cold-cathode flat panel displays and various vacuum microelectronic devices because of their excellent field emission properties, i.e., good emission stability, long emitter lifetime, and relatively low threshold voltage[Heer 1995-1179; Saito 2000-169; Jonge 2002-393]. For the practical application to field emission displays (FEDs), it is necessary to realize the growth of vertically aligned CNT arrays on a large area with suitable tube density and tube dimensions. In recent years, template methods, such as anodic aluminum oxide (AAO) nano-templates in particular, have been widely introduced to produce well aligned and mono-dispersed CNT arrays[Kyotani 1996-2109; Li 1999-367; Suh 1999-2047; Yuan 2001-3127; Bae 2002-277]. By electrochemical anodization of aluminum in an acidic electrolyte, one can obtain the nanoporous AAO template consisted of vertical pore channel arrays with a hexagonally close-packed (hcp) arrangement[Jessensky 1998-1173]. The diameter, the length, and the density of nanopores can be controlled by adjusting the anodizing conditions[Li 1998-6023], making AAO an ideal template for fabricating ordered arrays of nanostructured materials.

As the AAO is used as the template to grow CNTs without the catalyst, the diameter, the length, the arrangement, and the packing density of aligned nanotubes can faithfully replicate the pattern of the AAO nanopore structure. However, the obtained tubes are very poor in graphitization[Kyotani 1996-2109; Sui 2001-1523]. When the transition metal catalyst is pre-deposited at the AAO pore bottom for the CNT growth, the crystallinity of the metal-catalyzed tubes can be appreciably improved, but the relatively high tube growth rate will lead to overgrowth and entanglement of the dense tubes[Lee 2001-2387; Jeong 2002-1859]. For such a high density CNT array, the significant electrostatic screening effect

caused by the proximity of neighboring tubes would reduce the field enhancement and thus the emitted current[Nilsson 2000-2071]. Suh *et al*.[Suh 2002-2392] reported that the screening effect was minimal when the intertube distance was similar to the tube length overgrown from the AAO surface. In order to alleviate the screening effect, the nanotubes with a lower tube number density is favorable. Several methods, such as electron-beam lithography[Ren 1999-1086], micro contact printing[Nilsson 2000-2071], shadow mask[Fan 1999-512], and pulse-current electrochemical deposition[Tu 2002-4018], have been proposed to control the catalyst site density aiming at the reduction of the CNT density. However, only a few research focus on the control of the tube number density of CNTs grown on AAO templates[Jeong 2002-4003]. In this study, a simple and reliable method has been proposed to control the CNT density on the AAO template by regulating the flow rate ratio of CH_4 and H_2 precursor gases during the CNT growth. It was found that the tube number density of the aligned CNT arrays decreases linearly with increasing the CH_4 concentration, and thereby field emission characteristics of CNTs can be adjusted.

6.2 Mechanisms for tube density control

In the experiment, the two-step anodization, which has been depicted in detail in Chapter 4, was used to prepared ordered pore channel arrays of AAO. The cobalt catalyst for the CNT growth was electrochemically deposited at the pore bottom. The CNT growth was carried out in the microwave plasma (2.45 GHz) electron cyclotron resonance chemical vapor deposition (ECR-CVD) system which is schematically shown in Figure 3-3. The gas mixture of CH_4 and H_2 was used as the carbon source. The total

Table 6-1 Experimental conditions for the CNT density control on AAO template.

Sample	A	B	C
Microwave power	700 W	700 W	700 W
Substrate bias	-150 V	-150 V	-150 V
Working pressure	2 mTorr	2 mTorr	2 mTorr
Deposition temperature	600 °C	600 °C	600 °C
CH_4 flow rate	2 sccm	11 sccm	20 sccm
H_2 flow rate	20 sccm	11 sccm	2 sccm
CH_4 concentration	9%	50%	91%
Growth time	30 min	30 min	30 min

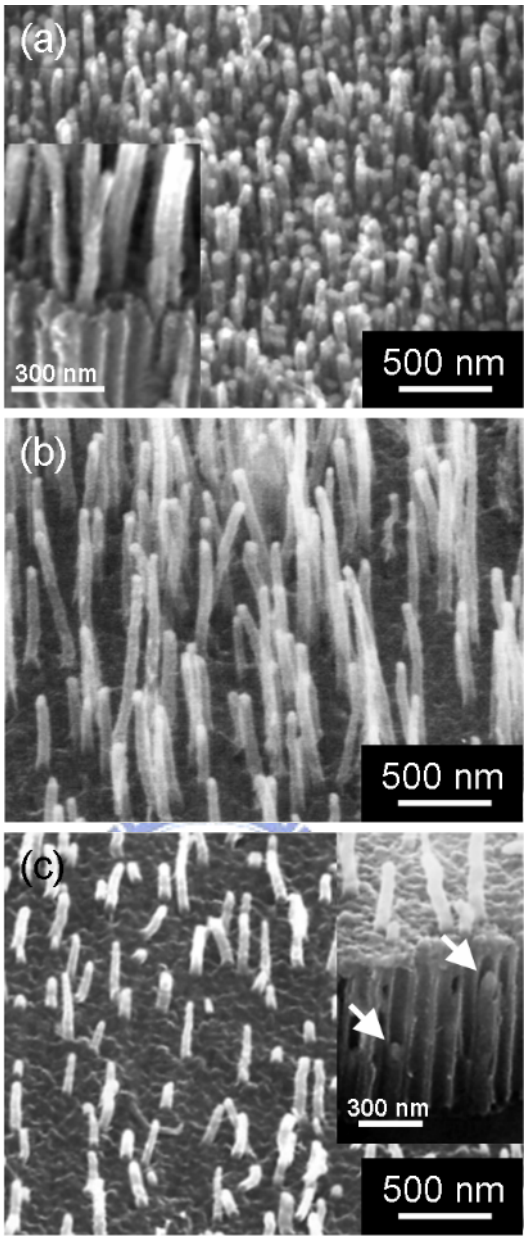

Figure 6-1 Side-view FE-SEM images of the cobalt-catalyzed CNTs on AAO template grown at CH_4 concentrations of (a) 9% (sample A), (b) 50% (sample B), and (c) 91% (sample C). The insets show the close-up view of the CNTs grown out of the AAO nanopores.

gas flow rate was kept constant at 22 sccm. The CH_4 concentration in the gas precursor was varied from 9 to 91% in order to investigate the influence of the CH_4:H_2 ratio on the CNT growth. The detailed conditions for the synthesis of CNTs on AAO template are summarized in Table 6-1.

Figure 6-1 shows the side-view field-emission scanning electron microscopy (FE-SEM) (Hitachi S-4000) images of the cobalt-catalyzed CNTs on the AAO template grown at different CH_4 concentrations. The FE-SEM observation of these samples exhibits that the CNT density significantly relies on the CH_4:H_2 feed ratio. Following

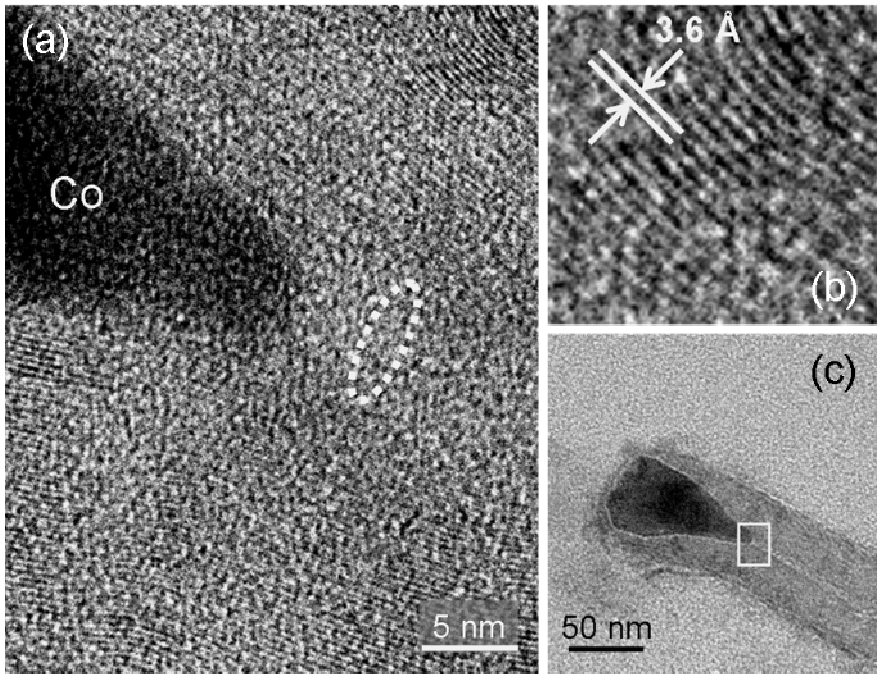

Figure 6-2 (a) HRTEM image of a cobalt-catalyzed CNT shown in Figure 6-1(b). The hollow core is indicated by a dashed ellipse. (b) is the enlarged picture of the tube wall. (c) is a corresponding low magnification TEM image. The square presents the magnified area of the HRTEM image.

the increase of the carbonaceous gas content, the number of nanotubes grown over the AAO nanopores decreases gradually. At the CH_4 concentration of 9% [see Figure 6-1(a)], the tube number density of CNT is as high as 9.0×10^9 tubes/cm^2, indicating a tube filled ratio in pores of about 82% (AAO pore density about 1.1×10^{10} pores/cm^2). In an extremely high CH_4 concentration of 91% [see Figure 6-1(c)], the observed tube number density decreases significantly to about 2.0×10^9 tubes/cm^2, corresponding to tube filled ratio of about 18%. These figures also reveal that the nanotubes confined by the AAO nanopores are uniform in diameter and tend to be vertically aligned. Figure 6-2(a) is the high-resolution transmission electron microscopy (HRTEM) (JEOL JEM-2010F) image of the nanotube shown in Figure 6-1(b). Because the tube has a relatively large diameter, only a part of the tube is shown in this figure. The multi-walled tube is composed of about 70-80 well-ordered graphitic walls and a 7-nm-wide hollow core. The inter-wall distance (d_{002}) is approximately 3.6 Å [see Figure 6-2(b)]. Figure 6-2(c) shows that a cobalt catalyst particle is encapsulated at the tip of tube and covered by graphitic cap, indicating that the CNT growth is cobalt-catalyzed and by means of the tip-growth mechanism[Baker 1989-315; Helveg 2004-426].

While the cobalt-catalyzed CNTs are grown on the AAO template, the nanotube growth and the carbon deposition on the AAO pore wall take place simultaneously[Jeong

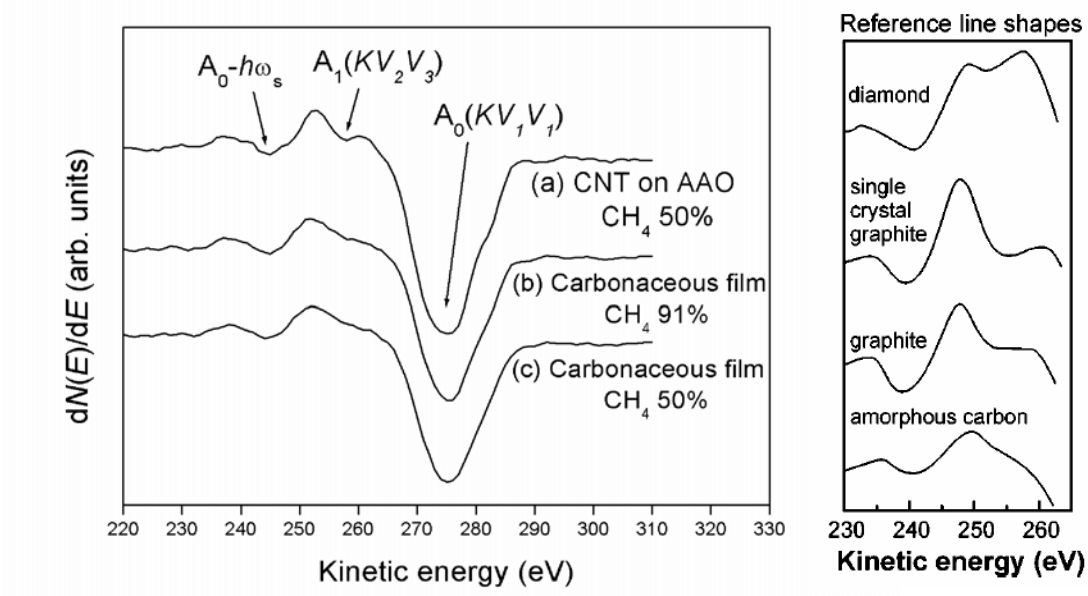

Figure 6-3 Graphitic Auger carbon (*KVV*) peaks of (a) an AAO assisted CNT grown at 50% CH_4, (b) the deposited carbonaceous film on the AAO surface grown at 91% CH_4, and (c) 50% CH_4. Reference line shapes of diamond, graphite, and amorphous carbon are provided for comparison[Teo 2002-116].

2001-2052]. As shown in Figure 6-1(c), the AAO surface appears to be covered with a thin layer of carbonaceous deposit, which blocks the outgrowth of most CNTs. In order to investigate the chemical nature of carbon in the nanotube and the deposit, Auger electron spectroscopy (AES) analyses were performed using a VG Microlab 310F Auger system with a Schottky field emission electron source. Figure 6-3 shows the carbon (*KVV*) Auger signals of the AAO templated CNTs and the deposited films on the AAO surface. By carefully analyzing the carbon (*KVV*) Auger line shape, one can obtain qualitative insight into the bonding structure of carbon atoms in carbon-based materials, such as diamond, graphite, and amorphous carbon[Steffen 1991-3981]. The carbon Auger signal shown in Figure 6-3(a) with a peak situated near 260 eV indicates that the carbon of CNT produced in this study is predominantly well-crystallized sp^2-bonded (crystalline graphite-like). For the area covered by the carbonaceous deposit, the KV_2V_3 trough located at 258 eV becomes vague [see Figure 6-3(b) and 6-3(c)], implying that the films mainly consist of amorphous carbon. These amorphous carbon layers, which are the byproduct of the CNT growth, are formed by the plasma decomposition of CH_4 and H_2 gases and condensed on the AAO surface. As the synthesis continues, it will gradually cover up the AAO nanopores and prevent the nanotubes from growing out of the nanopores. Therefore, in this study, the amorphous carbon byproduct seems to play an important role in the control of the tube number density of CNTs grown on the AAO

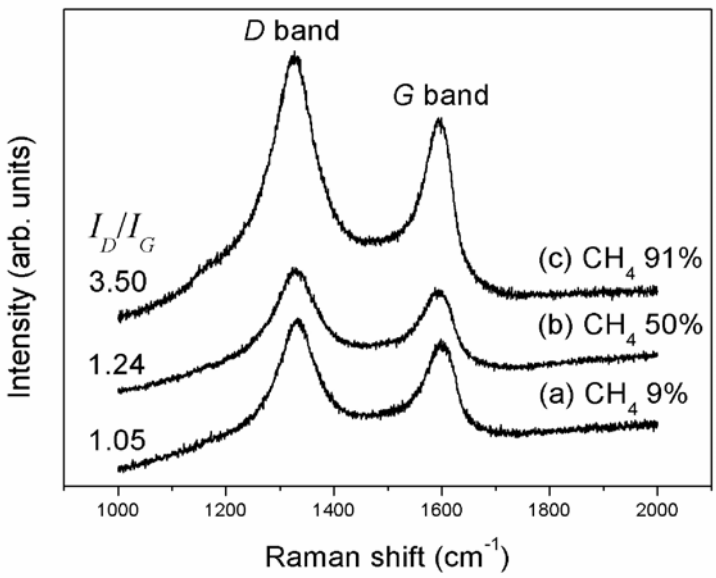

Figure 6-4 Raman spectra of the AAO assisted CNTs grown at (a) 9% CH_4, (b) 50% CH_4, and (c) 91% CH_4. The labeled value of I_D/I_G ratio is estimated in terms of the integral intensity.

template.

The structural characterization of the samples was studied by Raman spectroscopy. Figure 6-4 shows Raman spectra of the samples shown in Figure 6-1. Unpolarized visible Raman spectra were excited with the 632.8 nm line of a He-Ne laser and measured with the Jobin Yvon LABRAM HR Micro-Raman system. As shown in Figure 6-4, all spectra show two prominent bands located at approximately 1330 cm^{-1} (*D* band) and 1590 cm^{-1} (*G* band). The *G* band relating to the vibration of sp^2-bonded carbon atoms in a 2-dimensional hexagonal lattice indicates the presence of crystalline graphitic carbon atoms[Kasuya 1997-4434]. The *D* band originates from vibrations of carbon atoms with dangling bonds in plane terminations of disordered graphite or glassy carbons. In general, the intensity of the *D* band increases with an increase in the amount of unorganized carbon in samples or a decrease in graphite crystal size[Nemanich 1979-392]. The ratio of the integral intensities of the *D* and *G* bands, I_D/I_G, in this case is estimated as an indication of the deposition amount of the amorphous carbon byproduct. In Figure 6-4, it is found that the I_D/I_G ratio increases significantly with increasing the CH_4 concentration, suggesting that the amount of amorphous/disordered carbon atoms increases markedly as the CH_4:H_2 feed ratio increases[Ferrari 2000-14095]. This phenomenon is in agreement with the FE-SEM observations shown in Figure 6-1 and correlates closely with the etching effect induced by H_2 in plasma. During the CNT growth in the CH_4/H_2 plasma, the amorphous carbon byproduct is deposited on the substrate surface,

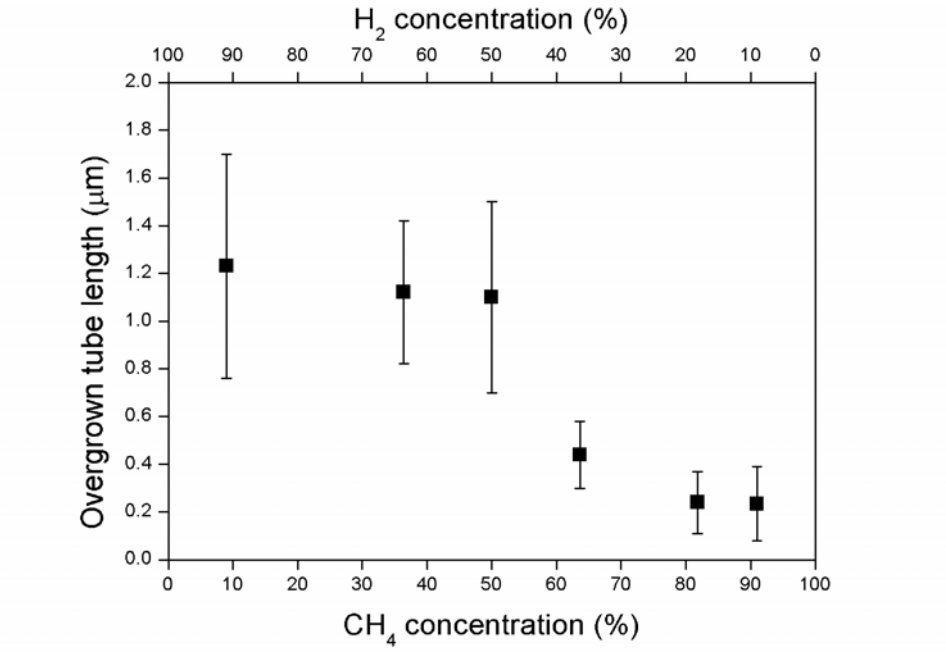

Figure 6-5 Overgrown tube length from the AAO surface as a function of CH_4 and H_2 concentrations.

whereas reactive hydrogen species in the plasma can also etch away the amorphous byproduct simultaneously[Kuttel 1998-2113]. If a high H_2 concentration is used, the substrate surface would almost free from the amorphous carbon since it is quickly etched away by the hydrogen species. In contrast, if a high CH_4 concentration is used, the amorphous carbon deposition predominates over the etching action, resulting in the continuing growth of the amorphous carbon. This eventually leaves the substrate surface covered with an amorphous carbon layer as shown in Figure 6-1(c). A considerably high I_D/I_G ratio of about 3.50 was detected for the growth condition of 91% CH_4.

The CH_4:H_2 flow ratio of the gas precursor decisively affects not only the deposition of the amorphous carbon byproduct but also the growth rate of CNTs. As clearly seen in Figure 6-1, after the CNT growth for 30 min, the nanotubes grown at a CH_4 concentration of 91% are obviously shorter than that grown at 50% and 9%. Figure 6-5 plots the overgrown tube length from the AAO surface against the CH_4 and H_2 concentrations. Increasing the CH_4 content tends to reduce the tube length. However, for CNT growth with the CH_4 concentrations below 50%, the obtained tube lengths depend weakly on the CH_4 concentration. This is due to that after the CNTs were grown to these lengths the activation of the cobalt catalyst was probably lost (poisoned[Qian 2003-878]) and the CNT growth was terminated. Even if the growth time was increased further, the nanotubes did not grow anymore. Here, we propose a possible mechanism for the reduction of the tube growth rate. It is well known that the H_2 content in the plasma can

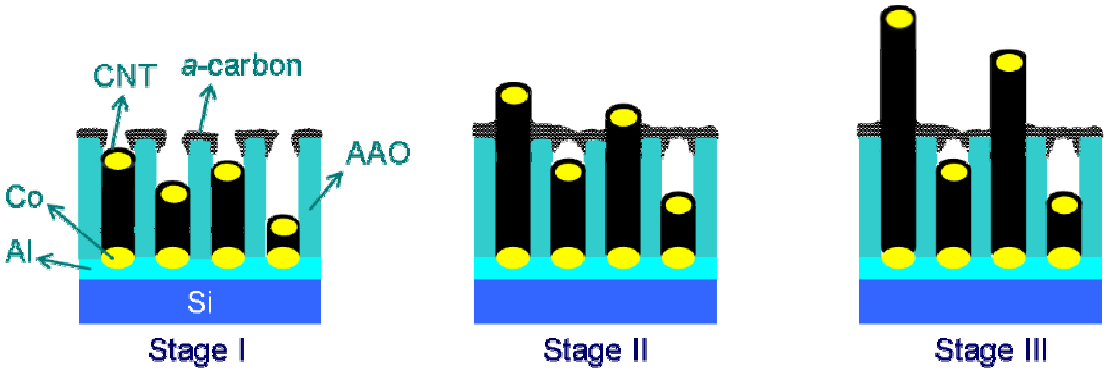

Figure 6-6 Schematic illustration of the growth model for the AAO template assisted CNTs. Stage 1: The CNT growth and the amorphous carbon deposition on AAO surface proceed simultaneously. Stage 2: Some short CNT without growing out from AAO pores punctually would be sealed inside the pores. Stage 3: Overgrown CNTs continuously grow up, and the sealed CNTs stop growing due to that the diffusion path of carbon source is blocked.

effectively promote the decomposition of CH_4 gas[Choi 2000-1864]. During the CNT growth, carbonaceous reactive species needed for CNT growth, such as CH_4 radicals, can be generated by hydrogen abstraction reactions[Truong 1994-8014] and then decomposed by the transition metal catalyst. These reactive species will eventually initiate the formation of CNTs. A large content of H_2 in the plasma can efficiently decompose the CH_4 gas, resulting in a large amount of the carbonaceous reactive species and thus a high CNT growth rate. Therefore, in our results, the tube growth rate was decreased significantly following the increase of the CH_4:H_2 feed ratio, which is essentially a consequence of decreasing the CH_4 decomposition efficiency. Besides, in the growth condition of a high CH_4:H_2 ratio, the large amount of amorphous carbon sediment may also be deposited on the CNT tip, which will hinder the diffusion of carbonaceous reactive species to the cobalt catalyst and consequentially reduce the tube growth rate.

The density control of CNTs grown on the AAO template can be achieved by directly tuning the CH_4:H_2 feed ratio during the CNT growth. We propose the following growth model for the AAO templated CNTs to explain the tube density control, as shown in Figure 6-6. When a high CH_4:H_2 feed ratio is used, the deposition of the amorphous carbon byproduct proceeds quickly and the CNT growth is retarded in terms of the tube length as indicated in Figure 6-5, causing that most nanotubes are blocked inside the nanopores by the amorphous carbon sediment and unable to grow out. As shown in the inset of Figure 6-1(c), some short nanotubes marked by white arrows were buried inside the nanopores. Nevertheless, the CNTs, which have already sprouted out of the nanopores, can continuously grow since the CNT growing site is at the tip of the

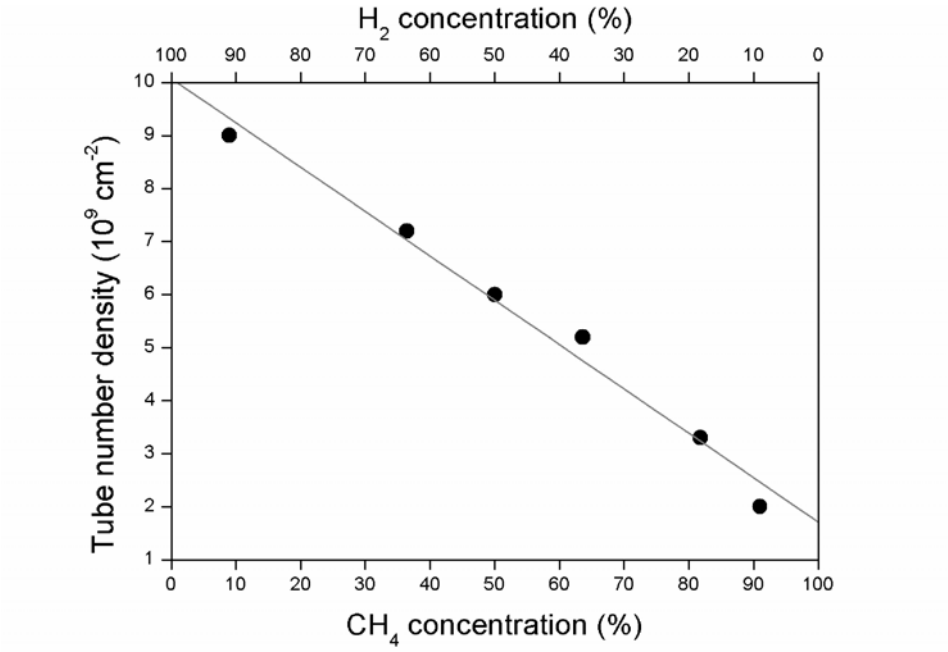

Figure 6-7 Tube number density of CNTs overgrown from AAO template as a function of CH_4 and H_2 concentrations.

tubes (tip-growth mechanism). With a high CH_4 concentration of 91%, only about 18% of CNTs could grow out from the nanopores. On the other hand, in a low CH_4:H_2 feed ratio, the AAO surface is almost free from the amorphous carbon [see the inset of Figure 6-1(a)] because the etching effect caused by hydrogen species is dominant, and CNTs can grow fast, leading to a very high tube number density. In this context, the number of CNTs grown over the AAO nanopores is strongly influenced by the CH_4:H_2 feed ratio. Figure 6-7 plots the tube number density of CNTs overgrown from the AAO template as a function of the CH_4 and H_2 concentrations. It nearly presents an inverse proportional relation between the tube number density and the CH_4 concentration. The tube density decreased 4.5 times in magnitude, and the corresponding tube filled ratio in the AAO nanopores decreased from 82 to 18%, when the CH_4 concentration increased from 9 to 91%.

6.3 Field emission of tube density controlled CNTs

Figure 6-8 shows the field emission current density (J) as a function of the applied electric field (E) for the AAO templated CNTs with three different tube densities shown in Figure 6-1. Measurements were conducted by the simple diode configuration and performed in a vacuum about 10^{-6} Torr. The distance between the CNTs and the anode was about 100 μm. The CNT film with the highest density of 9.0×10^9 tubes/cm^2

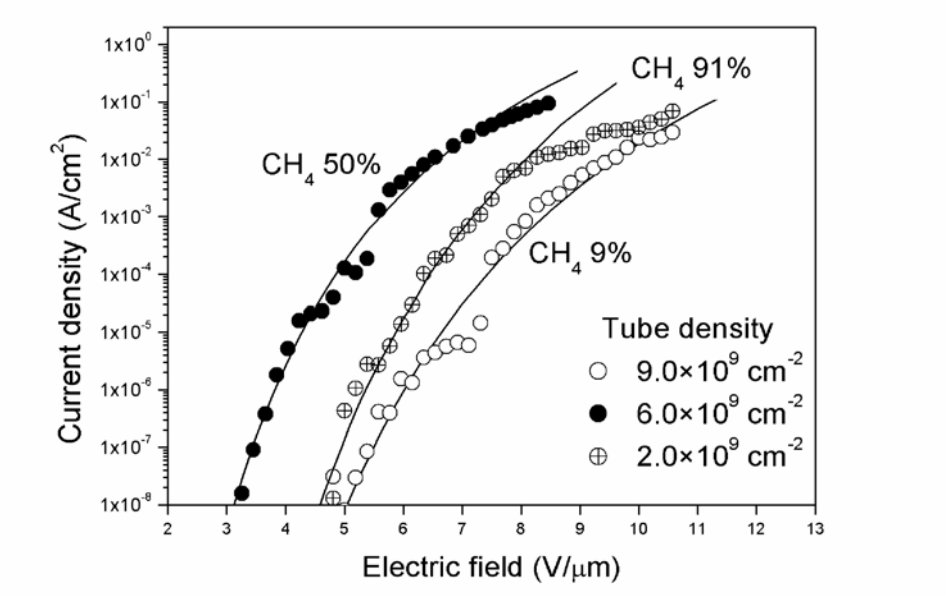

Figure 6-8 Field emission current density as a function of electric field for the CNTs grown on the AAO template with the three different tube densities shown in Figure 6-1. The solid curves are Fowler-Nordheim fits using the low current/field regions which do not show saturation.

shows the worst emission property in terms of the highest turn-on electric field (E_{to}) (about 8.1 V/μm) and the lowest current density, where E_{to} is defined herein as the electric field required to produce an emission current density of 1 mA/cm^2. As the tube density decreases to about 6.0×10^9 tubes/cm^2, the field emission property is remarkably improved (E_{to} about 5.2 V/μm). However, when the tube density decreases further to about 2.0×10^9 tubes/cm^2 the field emission property deteriorates (E_{to} about 7.4 V/μm). The dependence of the emission current on the applied electric field for a tip emitter can be described via the Fowler-Nordheim (F-N) relation:

$$J \propto E_{loc}^2 \exp(-\frac{6.83\times10^9 \varphi^{3/2}}{E_{loc}}) \tag{6.1}$$

where E_{loc} is the effective local electric field at the tip, and φ is the local work function of the emitter tip. According to the relation, the emission current is only dependent on the local electric field at the emission site assuming a constant work function on the emitter tip. The local field depends on the applied bias (V) and the radius (R_t) of a free-standing emitter tip, yielding

$$E_{loc} = \frac{V}{\xi R_t} \tag{6.2}$$

where ξ is a geometric factor with a value between 1 and 5. According to the FE-SEM micrographs shown in Figure 6-1, the CNTs grown at different CH_4 concentrations show little difference in the tip radius and shape, and hence all the three CNT samples presumably have similar values of ξ and R_t. The three samples differ in morphology mainly by two parameters, the tube density and length. The better field emission characteristic of the CNT film deposited with 50% CH_4 compared with the sample with 9% CH_4 is probably due to a slighter field-screening effect[Nilsson 2000-2071]. However, it has been reported that a single CNT with a higher aspect ratio of the tube can have a larger field enhancement, and thus have a lower E_{to} and a higher emission current [Edgcombe 2001-857]. Because the CNT arrays were grown out of the AAO nanopore channels, the three samples have a similar tube diameter about 75 nm. The average tube lengths protruding out of the AAO surface are estimated to be 1230 nm, 1110 nm and 237 nm for CNTs grown with CH_4 concentrations of 9%, 50% and 91%, respectively. Thus the tube aspect ratios of the three CNT samples are 26.3, 24.7 and 13.0, respectively, when the height of the CNT portion imbedded in the AAO template, which is about 740 nm thick, is taken into account. According to the *J-E* curve shown in Figure 6-8, at applied fields below 6 V/μm, the emission current density difference between the two denser CNT samples is more than three orders. This is far more than expected for such a small difference in the aspect ratio between the two samples. The large differences in the E_{to} and the emission current density between the two samples can thus be attributed to the field-screening effect. Moreover, compared with the CNTs grown with 91% CH_4, the film with 9% CH_4 shows inferior field-emission characteristic in the low field regime. Because the film of the highest tube density has a higher aspect ratio, it would be expected to have better field emission characteristic if the field-screening effect were insignificant. Therefore the highest E_{to} and lowest emission current density of the CNT film deposited with 9% CH_4 suggests that the field-screening effect plays a significant role on the field emission property. On the other hand, although the higher tube aspect ratio of the CNT film deposited with 50% CH_4 may improve the field emission property as compared with the CNTs grown with 91% CH_4, the former has worse field-screening effect than the later due to the higher tube density. We believe that the amorphous carbon deposit on the CNT tip is likely a major factor deteriorating the field emission characteristic of the CNTs grown with 91% CH_4. Under the growth condition of a very high CH_4 concentration, the amorphous carbon may be heavily deposited not only on

the AAO surface but also the CNT surface. The amorphous carbon layers on the CNT could increase the energy barrier for tunneling electrons emitted from the CNT to

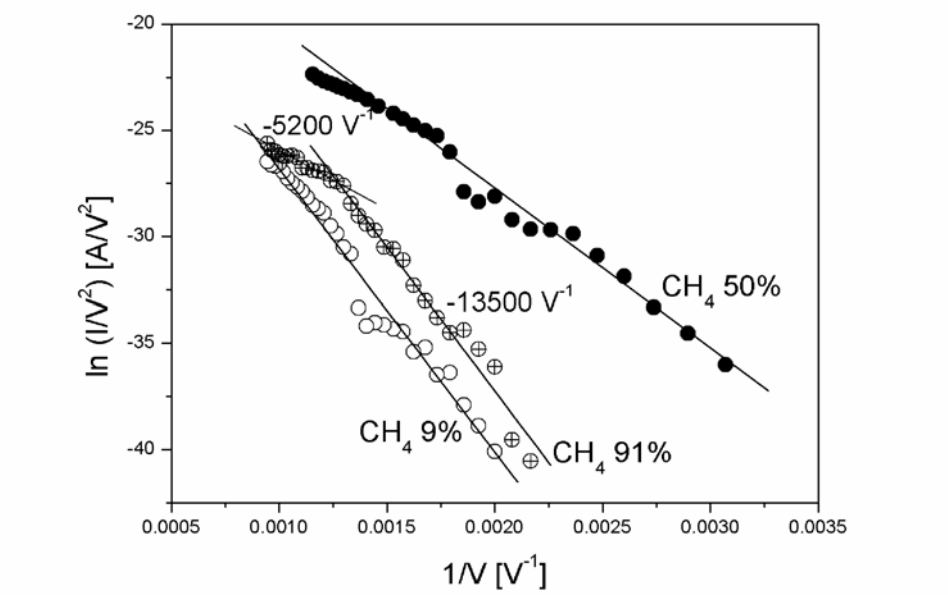

Figure 6-9 Corresponding Fowler-Nordheim plots of data shown in Figure 6-8. The slopes of the Fowler-Nordheim plot for the CNTs grown at 91% CH_4 are also indicated in the figure.

vacuum. Tanaka *et al*.[Tanaka 2004-864] reported that when a stand-alone CNT was covered with a thin amorphous carbon layer at its tip, the turn-on voltage for the field emission increased by 200 V and the increasing rate of the emission current with the voltage became smaller.

The F-N plot for the *J-E* curve of Figure 6-8 is shown in Figure 6-9. For the CNTs grown with 91% CH_4, the F-N plot clearly exhibits two linear segments with a slope of about -13,500 V^{-1} in the low field regime and a slope of about -5,200 V^{-1} in the high field regime. The other two CNT samples do not show such an obvious slope break although they also have a nonlinear feature in the F-N plots. Non-linearity of F-N plots for CNTs has been widely reported, and, in general, is ascribed to space charge effect resulting from ionization of residual gas molecules in the measurement vacuum chamber by the emitted electrons[Xu 2003-19], and/or energy barrier modification by an dielectric overlayer deposited on the CNTs during CNT growth[Tanaka 2004-864; Gao 2003-5602]. Defects in CNTs[Gao 2003-5602] and breakdown of the dielectric overlayer[Collins 1997-9391] are also proposed to be responsible for the nonlinear behavior. However, the three CNT samples probably have a comparable defect density because they were grown under a similar process condition except the CH_4:H_2 feed ratio. The breakdown of the dielectric overlayer is also excluded since the field emission result is reproducible. If the CNT tip

is heavily coated by the amorphous carbon deposit, the effective local work function and conductivity of the emitter can be significantly modified, resulting in a marked

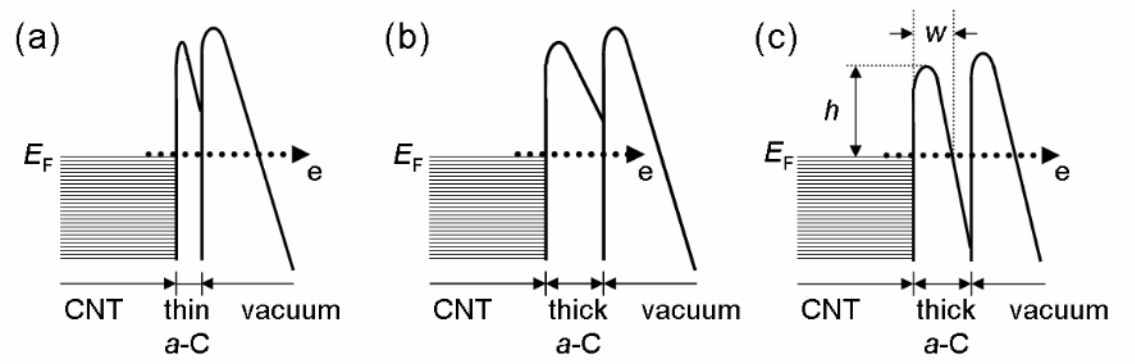

Figure 6-10 Schematic band diagram of the CNT tip with an amorphous carbon dielectric layer. (a) With a thin amorphous carbon layer at a low electric field, (b) thick amorphous carbon layer at a low electric field, and (c) thick amorphous carbon layer at a high electric field. E_F is the Fermi level of the CNT. *h* and *w* are the effective barrier height and barrier width of the dielectric layer, respectively.

deviation from the normal F-N plot. As discussed previously, during the CNT growth, amorphous carbon is deposited on the AAO surface and, possibly, the CNTs as well, and the amount of amorphous carbon deposit increases with increasing the CH_4 concentration in the gas mixture. The amorphous carbon overlayer on the nanotubes can modify the effective local work function of the CNT tips, and thus alter the field emission characteristic[Tanaka 2004-864]. For a very thin amorphous carbon overlayer, electrons emitted from the CNT can easily tunnel through the thin amorphous carbon dielectric layer under a moderate electric field, as shown in Figure 6-10(a). The work function modification on the emitter tip might just slightly alter the emission current and thus the E_{to}. But as the dielectric overlayer becomes thicker, the width of the energy barrier becomes wider, and thus electrons tunneling through the dielectric layer become difficult [Figure 6-10(b)]. Electrons emitted from CNT tips need overcome the extra energy barrier imposed by the amorphous carbon overlayer. A higher electric field is required to decrease the effective barrier height (*h*) and narrow the barrier width (*w*) so that electron tunneling and thus field emission can become thriving [Figure 6-10(c)]. Moreover, it has been reported that resistance present in the field emitter structure can lead to field emission degradation[Gröning 1999-1970]. If the emitter resistance or the emission current is large, a potential drop through the emitter will occur, lowering the local field at the emission site. This can cause deviation of the field emission from the normal F-N characteristic in the high emission current regime. Because significant amorphous carbon deposit is present on the CNT film grown with 91% CH_4, the

potential drop occurring through the dielectric overlayer at the emission site as field emission electrons leave CNT tips will be larger than that of the other two samples. This is probably an important reason why the CNT sample grown with 91% CH_4 has the F-N plot remarkably different from that of the other two samples, which have much less amorphous carbon deposit during the CNT growth.

6.4 Summary

A simple and reliable method has been presented to control the tube number density of aligned CNTs grown on the nanoporous AAO template. The key idea of this method is to take advantage of the competition between the growth of cobalt-catalyzed CNTs from the AAO pore bottom and the deposition of the amorphous carbon byproduct on the AAO nanoporous template. The number of CNTs grown over the nanopores is strongly depended on the flow rate ratio of CH_4 and H_2 in the precursor gas mixture during the CNT growth. It was found that the tube density of the CNT arrays on the AAO template decreases linearly with increasing the CH_4 concentration. By adjusting the CH_4:H_2 feed ratio, one can control the percentage of nanotubes overgrown out of the AAO nanopores from 82 to 18%. Although the amorphous carbon can effectively decrease the CNT density on the AAO template, thereby decreasing the field-screening effect and increasing the field enhancement, it notably deteriorates the electron field emission property of the CNTs. The nonlinearity of the F-N plot of the CNTs is ascribed to the deposition of the amorphous carbon overlayer on the CNT tip. The CNTs grown at 50% CH_4 show the best field emission property.